HHS Public Access

Author manuscript

Acad Radiol. Author manuscript; available in PMC 2016 April 01.

Published in final edited form as:

Acad Radiol. 2015 April ; 22(4): 467–474. doi:10.1016/j.acra.2014.11.007.

Performance Comparison of 1.5 T Endorectal Coil MRI with Non-Endorectal Coil 3.0 T MRI in Patients with Prostate Cancer

Zarine K. Shah, MD[1], **Saba N. Elias, MS**[1], **Ronney Abaza, MD**[3], **Debra L. Zynger, MD**[2], **Lawrence A. DeRenne, MD**[2], **Michael V. Knopp, MD, PhD**[1], **Beibei Guo, PhD**[4], **Ryan Schurr, BS**[5], **Steven B. Heymsfield, MD**[6], and **Guang Jia, PhD**[5,6,*]

[1]Department of Radiology, The Ohio State University, Columbus OH, USA

[2]Department of Pathology, The Ohio State University, Columbus OH, USA

[3]OhioHealth Dublin Methodist Hospital, Dublin, OH, USA

[4]Department of Experimental Statistics, Louisiana State University, Baton Rouge, LA, USA

[5]Department of Physics and Astronomy, Louisiana State University, Baton Rouge, LA, USA

[6]Pennington Biomedical Research Center, Baton Rouge, LA, USA

Abstract

Rationale and Objectives—To compare prostate morphology, image quality, and diagnostic performance of 1.5 T endorectal coil MRI and 3.0 T non-endorectal coil MRI in patients with prostate cancer.

Materials and Methods—MR images obtained of 83 patients with prostate cancer using 1.5 T MRI systems with an endorectal coil were compared to images collected from 83 patients with a 3.0 T MRI system. Prostate diameters were measured and image quality was evaluated by one ABR-certified radiologist (Reader 1) and one ABR-certified diagnostic medical physicist (Reader 2). The likelihood of the peripheral zone cancer presence in each sextant and local extent were rated and compared with histopathologic findings.

Results—Prostate anterior-posterior diameter measured by both readers was significantly shorter with 1.5 T endorectal MRI than with 3.0 T MRI. The overall image quality score difference was significant only for Reader 1. Both readers found that the two MRI systems provided similar diagnostic accuracy in cancer localization, extraprostatic extension, and seminal vesicle involvement.

Conclusion—Non-endorectal coil 3.0 T MRI provides prostate images that are natural in shape and that have comparable image quality to those obtained at 1.5 T with an endorectal coil, but not

*Address reprint requests to: Guang Jia, Department of Physics and Astronomy, Louisiana State University, Baton Rouge, LA, 70803. Phone: 225-334-2030, gjia@lsu.edu.

superior diagnostic performance. These findings suggest an opportunity exists for improving technical aspects of 3.0 T prostate MRI.

Keywords

prostate cancer; magnetic resonance imaging; image quality; endorectal coil; tumor localization; tumor staging

INTRODUCTION

Prostate cancer is the second most common cause of cancer death among American men. The American Cancer Society estimated that 233,000 new cases of prostate cancer would be diagnosed in 2014, and approximately 29,480 men would die of the disease (1). Magnetic resonance imaging (MRI), with excellent soft tissue contrast, provides high resolution images of the pelvis for use in prostate cancer management (2).

The use of an endorectal coil is an essential part of the prostate 1.5 T MRI protocol in the clinical diagnosis of prostate cancer (3). An endorectal coil is inserted tightly against the prostate during MRI examination in order to increase image resolution and improve staging accuracy (4). However, the endorectal coil leads to deformity in the prostate contour, and the anatomical distortion resulting from it can potentially hinder the diagnosis and pathology correlation (5). The changes in prostate shape and volume after the introduction of an endorectal coil may cause difficulties in MRI-computed tomography fusion and radiotherapy planning (6, 7). Another limitation is that patients with rectal stenosis or immediately after surgery or radiotherapy may not be good candidates for the use of the endorectal coil during MR examination (8).

MRI at 3.0 T is increasingly being used for routine clinical examinations (9). 3.0 T MRI has a nearly two-fold increase in signal-to-noise ratio compared to 1.5 T, with improved spatial resolution or shortened acquisition time (10). It is hypothesized that 3.0 T MRI of the prostate without the use of an endorectal coil may have the image quality and diagnostic accuracy equivalent to 1.5 T endorectal MRI (11, 12), while evaluating the prostate gland without anatomical distortion or compression (13).

The purpose of this study is to evaluate the effectiveness of 3.0 T MRI compared to 1.5 T endorectal MRI in assessing prostate morphology, image quality, and diagnostic performance in patients with prostate cancer.

MATERIALS AND METHODS

Study Design and Population

This study retrospectively accessed the American College of Radiology Imaging Network (ACRIN) #6659 trial (Prostate Cancer: Staging with MRI and MRS) with 1.5 T MRI using an endorectal coil (14), which was compared to our single institutional trial with 3T MRI using a phased-array coil (Figure 1). Our single institutional trial was approved by the local institutional review board and was compliant with the Health Insurance Portability and Accountability Act; informed consent was obtained from each patient. For image quality

assessment, we included consecutive prostate cancer patients (N = 83; mean age, 62 years; age range, 43–79 years; mean prostate-specific antigen, 9.4 ng/mL; range, 0.5–167.1 ng/mL) who underwent a 3.0 T MRI examination of the prostate between February 2009 and December 2012. We randomly selected a subset of 83 patients from ACRIN # 6659 trial (mean age, 57 years; age range, 39–69 years). For diagnostic performance assessment, the patients with both MRI and post-prostatectomy pathophysiological results were identified and included: N = 82 from ACRIN 6659 Trial and N = 69 from our single institutional trial.

MR Imaging Protocol

All ACRIN # 6659 trial MRI examinations were performed by using 1.5 T whole-body GE Healthcare MR units. Patients were imaged in the supine position with a pelvic/endorectal phased-array coil. A disposable expandable endorectal coil was used in combination with the phased-array coil at 1.5T. All in-house MR examinations were acquired on a 3.0 T MR system (Achieva, Philips Healthcare, Cleveland OH) using a 32-channel phased array coil in order to image the prostate in a natural shape without deformity usually caused by an endorectal coil. Images from both axial and coronal high-spatial-resolution turbo spin echo sequences were acquired (Table 1).

Image and Histopathology Analysis

All images were analyzed independently by two readers: one ABR-certified radiologist (Reader 1) with 11 years of clinical radiologic reading experience and one ABR-certified diagnostic medical physicist (Reader 2) with 8 years of prostate cancer MRI research experience. Images were reviewed on Philips Extended Brilliance Workspace (EBW) workstation at OSU (Columbus, OH) by Reader 1 and on GE Advantage Workstation (AW) at PBRC (Baton Rouge, LA) by Reader 2. The readers agreed in advance on prostate diameter measurement and the definition of image quality scores, as well as tumor localization and local extent.

Prostate left-right (LR) and anterior-posterior (AP) diameters were measured on axial T2-weighted images. Prostate LR diameter was defined as the longest left-to-right diameter in axial T2-weighted image; prostate AP diameter was defined as the AP diameter in the midline of the prostate in an axial T2-weighted image. Prostate cranial-caudal (CC) diameter was defined as the distance between the superior border of the prostate base and the bottom edge of the prostate apex in a coronal T2-weighted image. The ratio of LR diameter to AP and CC diameters were calculated for each patient.

Both readers independently scored the axial T2-weighted images based on four quality aspects: visualization of posterior border (score 5 to 1), seminal vesicles (SV) (score 5 to 1), neurovascular bundles (NVB) (score 4 to 1), and overall image quality (score 5 to 1). The higher score represented the most desirable imaging results (11) (summarized in Table 2). Both readers evaluated whether the axial T2-weighted images exhibited any artifacts that might affect diagnostic evaluation and briefly noted the type of artifacts (signal graininess, ghosting, coil-related SNR decrease, motion artifacts, etc.).

Both readers used axial T2-weighted images and a five-point scale to rate the likelihood of peripheral zone (PZ) cancer presence in each prostate sextant, with a score of 1 indicating

definitely no cancer, 2 unlikely cancer, 3 indeterminate cancer, 4 most likely cancer, and 5 certainly cancer. The readers also rated the likelihood of extraprostatic extension (EPE) and SV involvement using the same five-point scale as used for sextant cancer likelihood.

Whole-mount histopathology specimens were processed upon prostatectomy and analyzed by pathologists (14, 15). For our single institutional trial, two experienced Uro-pathologists reviewed the pathology slides independently of the clinical pathology reports (N=69). A pathology evaluation form and scoring system were used similar to the clinical pathology evaluation form used by the ACRIN trial (14). The prostates were divided into three schematic diagrams, with each appointed to the most representative slide for the apex, mid gland, and base, and another diagram for the SV. Each was divided into sextants and marked with the tumor location, site of EPE (if present), SV involvement, Gleason score, and tumor staging compliant with the guidelines of the College of American Pathologists Protocols (16). These forms were then translated into a scoring system with a score of 0 indicating no cancer, and 1 certainly cancer for prostate sextant, EPE presence, and SV involvement as the reference standard.

Statistical Analysis

Statistics for all continuous and ordinal data were reported as a mean ± standard deviation. The Hotelling's T-square multivariate test was used first to test the nine variables (five prostate diameter measurements and four imaging quality aspects) jointly between 1.5 T endorectal MRI and 3.0 T MRI. P-values for both Reader 1 and Reader 2 were less than 0.001, which indicated that there was at least one variable on which 1.5 T endorectal MRI and 3.0 T MRI differ. Consequently, the Mann-Whitney rank sum test was applied to each variable to test statistical significance. A P value of .05 or less was considered to indicate a statistically significant difference.

The diagnostic performance scoring results (cancer localization and local extent) were compared with pathology findings. The sensitivity, specificity, and area under the receiver operating characteristic curves (AUC) were computed. AUCs for 1.5 T Endorectal and 3.0 T were compared using bootstrap method (17).

RESULTS

Figure 1 shows the prostate diameters measured by two readers. LR diameter was the longest among the three diameters for both 1.5 T and 3.0 T for both readers. There was no significant difference in LR diameter between 1.5 T endorectal MRI and 3.0 T MRI for Reader 1 (Table 3). Prostate CC diameter was shorter than LR but longer than AP diameter for both readers at both magnetic field strengths. Prostate CC diameter was significantly shorter at 1.5 T endorectal MRI than 3.0 T only for reader 1 but not for Reader 2. Prostate AP diameter was significantly shorter at 1.5 T endorectal MRI than at 3.0 T MRI for both readers. LR/AP and LR/CC ratios at 1.5 T endorectal MRI were significantly larger than those at 3.0 T for both readers.

The majority of the subject MR examinations were scored highest by both readers for all four image quality aspects (Figure 3). For visualization of the posterior border, 3.0 T MRI

was scored significantly higher than 1.5 T endorectal MRI by Reader 1 only. For visualization of SV, 1.5 T endorectal MRI was scored significantly higher than 3.0 T MRI by Reader 2 only. There was no significant difference in visualization of NVB between 1.5 T endorectal and 3.0 T MRI for both readers. For overall image quality, the score difference was significant for Reader 1 only (Table 3).

Image artifacts were identified in 55.4% (46/83) of subjects with 1.5 T endorectal MRI by Reader 1, which is significantly greater than 9.6% (8/83) of subjects with 3.0 T MRI ($P < 0.001$). Reader 2 identified image artifacts in 51.8% (43/83) of subjects with 1.5 T endorectal MRI and 21.7% (18/83) of subjects with 3.0 T MRI ($P < 0.001$). The typical image artifacts from 1.5 T endorectal MRI included ghosting (Figure 4a), coil-related SNR decrease (Figure 4b), signal graininess, and prostate motion artifacts. The typical artifacts from 3.0 T MRI are signal graininess (Figure 4c), rectum motion artifact (Figure 4d), and breathing artifacts.

With six sextants analyzed per patient, and 82 patients (Reader 1 and 2) from 1.5 T endorectal and 68 patients (Reader 1, one case excluded due to dramatic motion artifact) and 69 patients (Reader 2) from 3.0 T, the final analysis included 1806 sextants. For both readers, 1.5 T endorectal MRI showed similar accuracy in PZ cancer localization as 3.0 T MRI (Table 3). Only Reader 2 gave higher but non-significant diagnostic accuracy in EPE at 1.5 T endorectal than at 3.0 T. Only Reader 1 gave higher but non-significant diagnostic accuracy in SV involvement at 3.0 T than at 1.5 T endorectal MRI, as shown in Figure 5.

DISCUSSION

Accurate prostate shape and size measurement is important in prostate cancer diagnosis and radiotherapy planning (7, 18). The shape of the prostate is less distorted when only external array is used (6, 18–20). An endorectal coil was shown to reduce prostate CC and AP diameters in our study, which can be justified by the expansion of the rectum (resulting in direct mechanical pressure on the prostate) due to endorectal coil insertion and coil balloon filling. LR/CC and LR/AP ratio showed a significant increase from 3.0 T to 1.5 T endorectal MRI, indicating the prostate deformation to a more flattened ellipsoid by the presence of an endorectal coil. Our results did not show prostate LR diameter reduction induced by an endorectal coil. An intra-patient comparison showed that the introduction of the endorectal coil significantly reduced all three diameters and the prostate volume, as well as the volumes of the central gland and peripheral zone (6, 18). Significant deformations in the shape of the whole prostate and peripheral zone caused by an endorectal coil have been observed (21). Prostate segmentation and image registration strategies have been proposed to resolve prostate deformation in endorectal MRI (13, 19, 22).

Although there is no mechanical pressure from an endorectal coil at 3.0 T non-endorectal MRI, gaseous distension may expand the rectum during examination, which can compress the prostate and result in prostate shape change. Repeated non-endorectal MRI examinations have revealed a significant prostate deformation that requires a deformable registration (23). Based on our experience, fleet enema before MR examination may not be efficient in controlling passing gas in rectum. A combination of a catheter, a hollow tube, and a rectal

obturator has been used to prevent gas buildup in the rectum at 0.5 T MRI (21). A simple and comfortable method for preventing gas buildup is crucial in order to efficiently minimize the degree of expansion of the rectum and its effect on prostate shape at 3.0 T non-endorectal MRI.

Image artifacts are reduced when only an external array is used. Image artifacts were noticed in more than half of the patients with endorectal MRI in this study, but only in 10% to 20% of the patients with non-endorectal MRI; this is similar to a previous report (8). The artifact of the endorectal coil-related SNR reduction in the study is also called a “coil flare artifact,” i.e. a flare of high signal intensity on the T2-weighted images at the interface of the endorectal coil and normal tissues (24). Another endorectal coil-related artifact is the ghosting artifact in the study, which has been defined by a straight line across the image at the anterior aspect of the balloon (24). The ghosting artifact can affect the visualization of the neurovascular bundles, which may explain the significant lower score of NVB visualization at endorectal MRI for Reader 1. Motion artifacts from the prostate, the rectum, or from breathing have been noticed in both non-endorectal and endorectal MRIs. These artifacts can significantly degrade the image and affect the visualization of the intra-prostatic tissues. The motion artifacts in non-endorectal MRI have been scaled to appear less significant than those in endorectal MRI (25). A periodically-rotated overlapping parallel lines with enhancing reconstruction (PROPELLER or BLADE) acquisition scheme (26) may help to reduce the motion artifacts in prostate T2-weighted images. Further optimization on BLADE is necessary in order to maintain high tumor-to-peripheral-zone contrast in the prostate.

Our study used the scoring system from a report by Sosna et al (11) for image quality analysis. Both readers in our report consistently gave the highest score (most desirable imaging results) for the majority of patients in all four aspects, which seems different from Sosna’s report. It is important for all readers to agree on the scoring definitions before their independent reading; however, it cannot guarantee that two reports will yield similar scores unless some typical cases could be shared and jointly reviewed as a benchmark. Reader 1 scored prostate posterior border visualization at 3.0 T, slightly but significantly higher than at 1.5 T endorectal MRI, which may be due to frequent ghosting artifacts induced by the endorectal coil at 1.5 T MRI. Reader 2 scored SV visualization at 3.0 T lower than at 1.5 T endorectal MRI, which might be due to more bowel peristalsis artifacts without fixation from the endorectal coil. For overall image quality, Reader 1 scored 3.0 T MRI significantly higher than 1.5 T endorectal MRI, which may have resulted from Reader 1 being more vigilant to image artifacts.

We used the same rating system in ACRIN # 6659 trial report (14) to rate the likelihood of the presence of peripheral zone cancer in each sextant by reading axial T2-weighted images. Both readers rated 3.0 T MRI without an endorectal coil as comparable to 1.5 T endorectal MRI. This is consistent with the reading results from the report by Turkbey, et al (27), who concluded that 3.0 T non-endorectal MRI tends to identify larger tumors but can miss smaller tumors. The visibility and delineation of smaller lesions will require a greater SNR and a higher spatial resolution, which could be achieved by combining the external array and the endorectal coil at 3.0 T. T2-weighted images with a voxel size of 0.375 × 0.625 × 1.5

mm for a voxel volume of 0.35 mm^3 (28), or 0.18 × 0.18 × 4 mm for a voxel volume of 0.13 mm^3 (29), have been demonstrated in order to show excellent anatomical detail and increased T2 contrast. These are superior to the T2-weighted images at 3.0 T non-endorectal MRI in the study (voxel size of 0.729 × 0.909 × 3 mm for a voxel volume of 1.99 mm^3).

Three reports have shown that both 1.5 T endorectal and 3.0 T MRI had a similar accuracy for the local staging of prostate cancer (8, 10, 12). Our analysis by both readers yielded non-significant results in terms of EPE and SV involvement for 1.5 T endorectal and 3.0 T MRI that have been noted in previous reports. For patients who require an accurate staging of their prostate cancer, integrated endorectal-pelvic phased-array coils may be used to improve the SNR (30) and image resolution (31), resulting in an improvement of EPE specificity (32) and enabling a delineation of minimal EPE as small as 0.5 mm (25).

We are aware that our study has some limitations. T2-weighted MR images at 3.0 T were acquired using a small FOV (140 × 140 mm^2), which may be suboptimal. Sosna et al compared the image quality of a smaller FOV (140 × 140 mm^2) and a larger FOV (160 × 160 mm^2) at 3.0 T; the latter was shown to have significantly better image quality (11). Although a 32-channel phased-array coil has been used at 3.0 T MRI, an emerging upgrade, the digital coil platform is supposed to improve SNR by up to 40% (33). Whether the digital coil platform could improve the detection and staging of prostate cancer still needs rigorous scientific evaluation. Another limitation is that only T2-weighted MRI was used in evaluating diagnostic performance. Multi-parametric imaging combining T2-weighted MRI and functional MRI and may provide better accuracy for tumor localization (34). It is impossible to do a blinded comparison of 1.5 T endorectal and 3.0 T since an endorectal coil significantly dilates the rectum and the circular shape of the rectum wall cannot not be missed on axial T2-weighted MR images. This could potentially create a negative bias against the endorectal technique. Finally, the two readers read the images on different workstations (Philips EBW and GE AW) and have different backgrounds (radiology and radiologic physics), which may partially contribute to the readers' inconsistence in the results.

In conclusion, 3.0 T MRI without an endorectal coil provides prostate images that are natural in shape and that have comparable image quality to those obtained at 1.5 T with an endorectal coil. The diagnostic performance of T2-weighted MR images at 3.0 T without an endorectal coil is not superior to 1.5 T endorectal MRI, a finding suggesting that an opportunity exists for improving technical aspects of 3.0 T prostate MRI.

Acknowledgments

Grant support: This study was supported in part by a grant from National Institutes of Health (U01CA080098-14, American College of Radiology Imaging Network Young Investigator Initiative Project Subaward #1117), a grant from the National Institutes of Health (R21CA156945), and a grant from the American Urological Association Foundation Research Scholars Program and EUSA Pharma (USA), Inc.

References

1. Siegel R, Ma J, Zou Z, Jemal A. Cancer statistics, 2014. CA Cancer J Clin. 2014; 64(1):9–29. [PubMed: 24399786]

2. Mazaheri Y, Shukla-Dave A, Muellner A, Hricak H. MRI of the prostate: clinical relevance and emerging applications. J Magn Reson Imaging. 2011; 33(2):258–74. [PubMed: 21274967]
3. Hricak H, Choyke PL, Eberhardt SC, Leibel SA, Scardino PT. Imaging prostate cancer: a multidisciplinary perspective. Radiology. 2007; 243(1):28–53. [PubMed: 17392247]
4. Hricak H, White S, Vigneron D, et al. Carcinoma of the prostate gland: MR imaging with pelvic phased-array coils versus integrated endorectal--pelvic phased-array coils. Radiology. 1994; 193(3): 703–9. [PubMed: 7972810]
5. Rajesh A, Coakley FV. MR imaging and MR spectroscopic imaging of prostate cancer. Magn Reson Imaging Clin N Am. 2004; 12(3):557–79. [PubMed: 15271371]
6. Heijmink SW, Scheenen TW, van Lin EN, et al. Changes in prostate shape and volume and their implications for radiotherapy after introduction of endorectal balloon as determined by MRI at 3T. Int J Radiat Oncol Biol Phys. 2009; 73(5):1446–53. [PubMed: 19036532]
7. Hensel JM, Menard C, Chung PW, et al. Development of multiorgan finite element-based prostate deformation model enabling registration of endorectal coil magnetic resonance imaging for radiotherapy planning. Int J Radiat Oncol Biol Phys. 2007; 68(5):1522–8. [PubMed: 17674983]
8. Park BK, Kim B, Kim CK, Lee HM, Kwon GY. Comparison of phased-array 3.0-T and endorectal 1.5-T magnetic resonance imaging in the evaluation of local staging accuracy for prostate cancer. J Comput Assist Tomogr. 2007; 31(4):534–8. [PubMed: 17882027]
9. Rouviere O, Hartman RP, Lyonnet D. Prostate MR imaging at high-field strength: evolution or revolution? Eur Radiol. 2006; 16(2):276–84. [PubMed: 16155721]
10. Beyersdorff D, Taymoorian K, Knosel T, et al. MRI of prostate cancer at 1.5 and 3.0 T: comparison of image quality in tumor detection and staging. Am J Roentgenol. 2005; 185(5): 1214–20. [PubMed: 16247137]
11. Sosna J, Pedrosa I, Dewolf WC, Mahallati H, Lenkinski RE, Rofsky NM. MR imaging of the prostate at 3 Tesla: comparison of an external phased-array coil to imaging with an endorectal coil at 1.5 Tesla. Acad Radiol. 2004; 11(8):857–62. [PubMed: 15354305]
12. Torricelli P, Cinquantini F, Ligabue G, Bianchi G, Sighinolfi P, Romagnoli R. Comparative evaluation between external phased array coil at 3 T and endorectal coil at 1.5 T: preliminary results. J Comput Assist Tomogr. 2006; 30(3):355–61. [PubMed: 16778606]
13. Tahmasebi AM, Sharifi R, Agarwal HK, et al. A statistical model-based technique for accounting for prostate gland deformation in endorectal coil-based MR imaging. Conf Proc IEEE Eng Med Biol Soc. 2012; 2012:5412–5. [PubMed: 23367153]
14. Weinreb JC, Blume JD, Coakley FV, et al. Prostate cancer: sextant localization at MR imaging and MR spectroscopic imaging before prostatectomy--results of ACRIN prospective multi-institutional clinicopathologic study. Radiology. 2009; 251(1):122–33. [PubMed: 19332850]
15. Jia G, Abaza R, Williams JD, et al. Amide proton transfer MR imaging of prostate cancer: a preliminary study. J Magn Reson Imaging. 2011; 33(3):647–54. [PubMed: 21563248]
16. Pantanowitz L, Sinard JH, Henricks WH, et al. Validating whole slide imaging for diagnostic purposes in pathology: guideline from the college of american pathologists pathology and laboratory quality center. Arch Pathol Lab Med. 2013; 137(12):1710–22. [PubMed: 23634907]
17. Robin X, Turck N, Hainard A, et al. pROC: an open-source package for R and S+ to analyze and compare ROC curves. Bmc Bioinformatics. 2011; 12:77. [PubMed: 21414208]
18. Wu X, Dibiase SJ, Gullapalli R, Yu CX. Deformable image registration for the use of magnetic resonance spectroscopy in prostate treatment planning. Int J Radiat Oncol Biol Phys. 2004; 58(5): 1577–83. [PubMed: 15050339]
19. Bharatha A, Hirose M, Hata N, et al. Evaluation of three-dimensional finite element-based deformable registration of pre- and intraoperative prostate imaging. Med Phys. 2001; 28(12): 2551–60. [PubMed: 11797960]
20. Pursley J, Risholm P, Fedorov A, et al. A Bayesian nonrigid registration method to enhance intraoperative target definition in image-guided prostate procedures through uncertainty characterization. Med Phys. 2012; 39(11):6858–67. [PubMed: 23127078]
21. Hirose M, Bharatha A, Hata N, et al. Quantitative MR imaging assessment of prostate gland deformation before and during MR imaging-guided brachytherapy. Acad Radiol. 2002; 9(8):906–12. [PubMed: 12186439]

22. Schreibmann E, Xing L. Narrow band deformable registration of prostate magnetic resonance imaging, magnetic resonance spectroscopic imaging, and computed tomography studies. Int J Radiat Oncol Biol Phys. 2005; 62(2):595–605. [PubMed: 15890605]
23. Brock KK, Nichol AM, Menard C, et al. Accuracy and sensitivity of finite element model-based deformable registration of the prostate. Med Phys. 2008; 35(9):4019–25. [PubMed: 18841853]
24. Husband JE, Padhani AR, MacVicar AD, Revell P. Magnetic resonance imaging of prostate cancer: comparison of image quality using endorectal and pelvic phased array coils. Clin Radiol. 1998; 53(9):673–81. [PubMed: 9766721]
25. Heijmink SW, Futterer JJ, Hambrock T, et al. Prostate cancer: body-array versus endorectal coil MR imaging at 3 T--comparison of image quality, localization, and staging performance. Radiology. 2007; 244(1):184–95. [PubMed: 17495178]
26. Rosenkrantz AB, Bennett GL, Doshi A, Deng FM, Babb JS, Taneja SS. T2-weighted imaging of the prostate: Impact of the BLADE technique on image quality and tumor assessment. Abdom Imaging. 2014
27. Turkbey B, Merino MJ, Gallardo EC, et al. Comparison of endorectal coil and nonendorectal coil T2W and diffusion-weighted MRI at 3 Tesla for localizing prostate cancer: Correlation with whole-mount histopathology. J Magn Reson Imaging. 2013
28. Bloch BN, Rofsky NM, Baroni RH, Marquis RP, Pedrosa I, Lenkinski RE. 3 Tesla magnetic resonance imaging of the prostate with combined pelvic phased-array and endorectal coils; Initial experience. Acad Radiol. 2004; 11(8):863–7. [PubMed: 15288036]
29. Futterer JJ, Scheenen TW, Huisman HJ, et al. Initial experience of 3 tesla endorectal coil magnetic resonance imaging and 1H-spectroscopic imaging of the prostate. Invest Radiol. 2004; 39(11): 671–80. [PubMed: 15486528]
30. Kim DY, Schnall MD, Rosen MA, Connick T. Prostate MR imaging at 3T with a longitudinal array endorectal surface coil and phased array body coil. J Magn Reson Imaging. 2008; 27(6): 1327–30. [PubMed: 18504745]
31. Futterer JJ, Heijmink SW, Scheenen TW, et al. Prostate cancer localization with dynamic contrast-enhanced MR imaging and proton MR spectroscopic imaging. Radiology. 2006; 241(2):449–58. [PubMed: 16966484]
32. Futterer JJ, Engelbrecht MR, Jager GJ, et al. Prostate cancer: comparison of local staging accuracy of pelvic phased-array coil alone versus integrated endorectal-pelvic phased-array coils. Local staging accuracy of prostate cancer using endorectal coil MR imaging. EurRadiol. 2007; 17(4): 1055–65.
33. Serai SD, Merrow AC, Kline-Fath BM. Fetal MRI on a multi-element digital coil platform. Pediatr Radiol. 2013; 43(9):1213–7. [PubMed: 23649206]
34. Dickinson L, Ahmed HU, Allen C, et al. Magnetic resonance imaging for the detection, localisation, and characterisation of prostate cancer: recommendations from a European consensus meeting. Eur Urol. 2011; 59(4):477–94. [PubMed: 21195536]

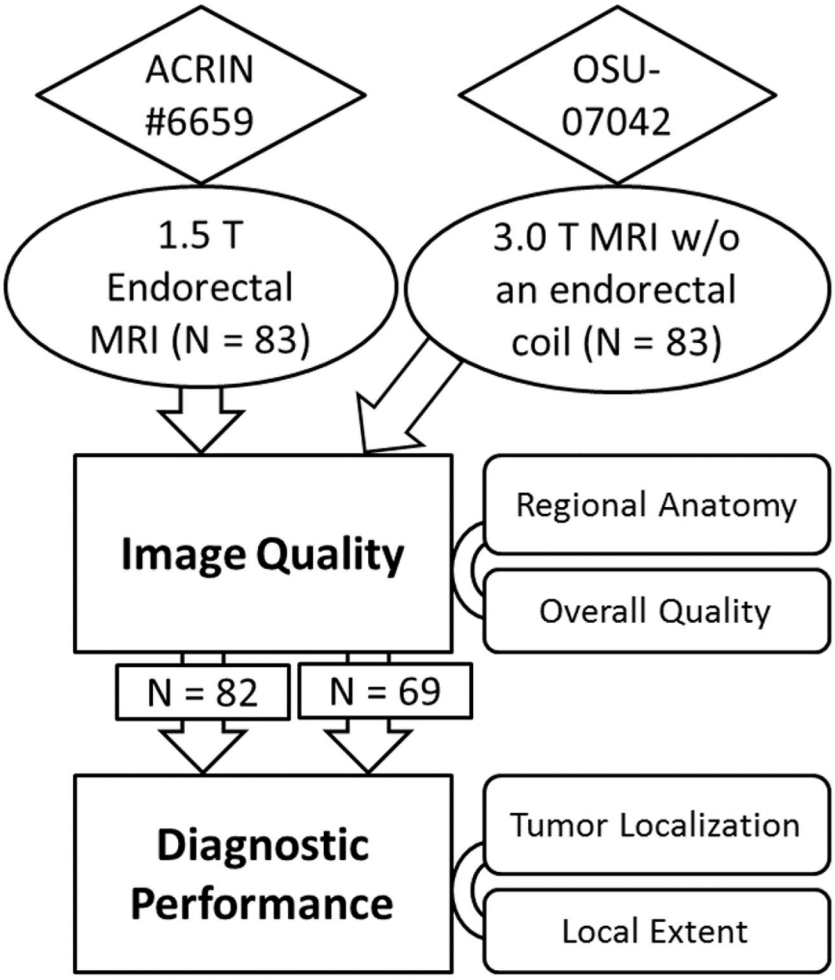

Figure 1.

Research design flow chart. In order to evaluate whether 3.0 T MRI without an endorectal coil is clinically usable, the ACRIN imaging archive with endorectal 1.5 T MRI was compared to our in-house 3.0 T MR imaging study without an endorectal coil.

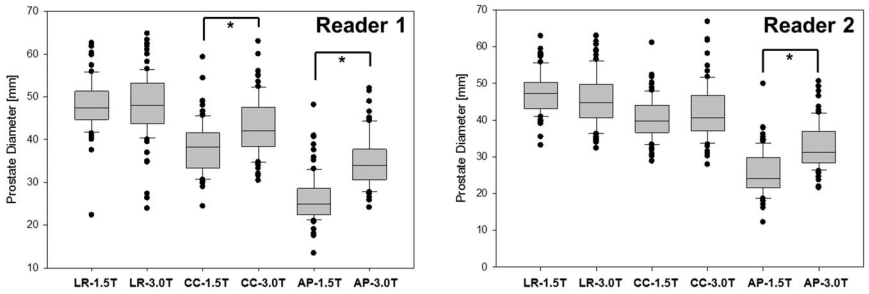

Figure 2.

Prostate diameter measurement results by 2 readers. LR diameter was generally the longest, and AP shortest, among the three diameters. AP diameter at 1.5 T endorectal MRI was significantly shorter than that at 3.0 T due to the rectum dilation for an endorectal coil insertion and fixation as reviewed by both readers.

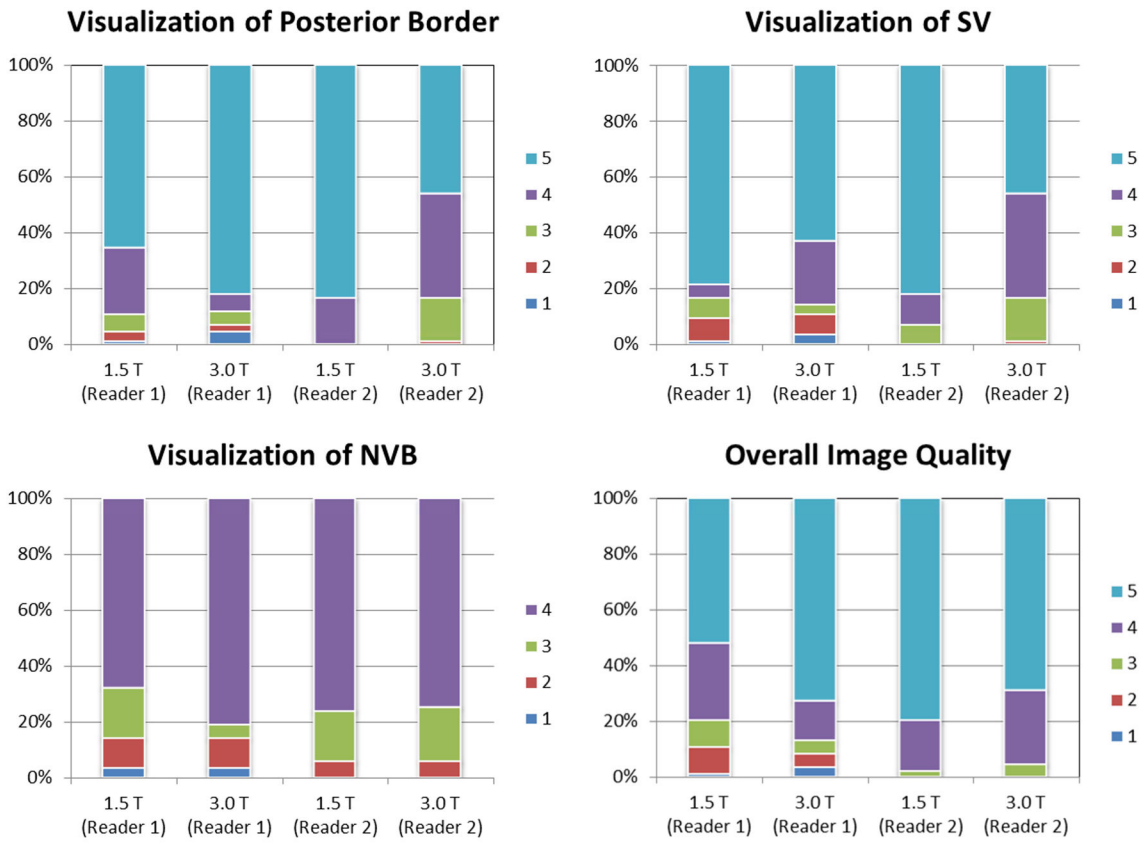

Figure 3.

100% stacked column plot shows the percentage of subjects with different scores, as evaluated by two readers. Highest score was given to the majority of subjects at either 1.5 T endorectal or 3.0 T MRI.

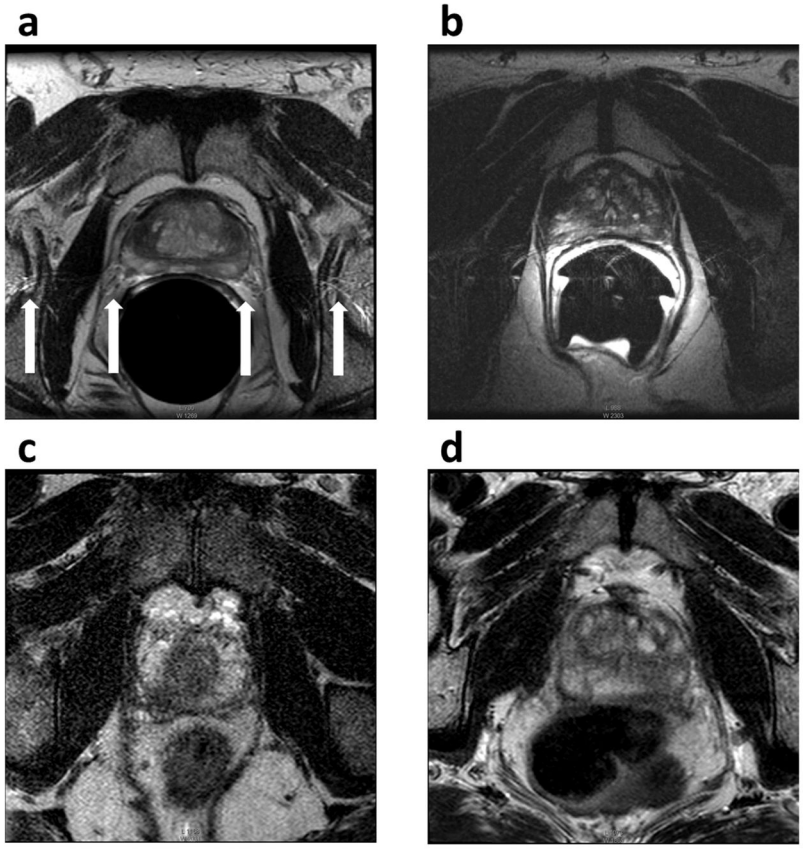

Figure 4.

Image artifacts on 1.5 T endorectal and 3.0 T MRI. The typical image artifacts from 1.5 T endorectal MRI included ghosting (a) and coil-related SNR decrease (b). The typical artifacts from 3.0 T MRI are signal graininess (c) and rectum motion artifact (d).

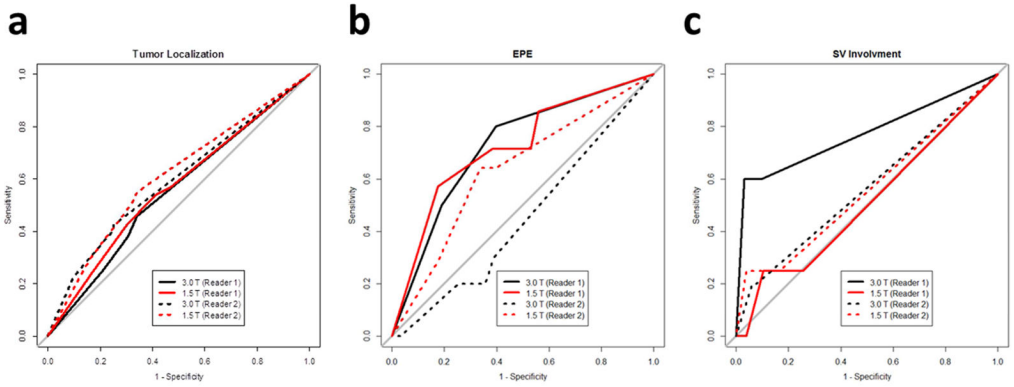

Figure 5.

Receiver operating characteristic curves of 1.5 T endorectal MRI diagnostic performances versus 3.0 T MRI performances for both readers in tumor localization (a), extraprostatic extension (b), and seminal vesicle involvement (c).

Table 1

Parameters for T2-weighted MR Imaging

Parameters	Axial T2-weighted Fast Spin Echo		Coronal T2-weighted Fast Spin Echo	
	1.5 T Endorectal	3.0 T	1.5 T Endorectal	3.0 T
Coil	Torso phased-array, endorectal	32-channel phased-array	Torso phased-array, endorectal	32-channel phased-array
TR (ms)/TE (ms)	4000–6600/90–150	3488–4400/100	4000–6500/90–150	2138–2685/100
Section thickness	3	3	3	3
Intersection gap (mm)	0–1	0.3	0–1	0.5
Field of view (mm)	100–142	140	100–140	260
Frequency direction	Anteroposterior	Anteroposterior	Anteroposterior or superoinferior	superoinferior
Matrix	256 × 192	192 × 154	256 × 192	304 × 294
Number of signals acquired	1.5–2	2	1.5–3	2
Echo train length	8–16	14	8–16	14

Notes: TR = repetition time, TE = echo time

Table 2

Qualitative Evaluation of Image Quality

Visualization of Posterior Border (PB)	Visualization of Seminal Vesicles (SV)
5. Well delineated	5. Margins and septations seen
4. 75–100% of margin clearly seen	4. Margins seen, septations poorly defined
3. 50–75% of margin clearly seen	3. Septations seen, margins poorly defined
2. 25–50% of margin clearly seen	2. Poorly defined
1. <25% of margin clearly seen	1. Unreadable

Visualization of Neurovascular Bundle (NVB)	Overall Image Quality Rating
4. Seen well on both sides	5. Excellent
3. Seen well on one side	4. Very good
2. Seen suboptimally on both sides	3. Good
1. Unreadable	2. Fair

TABLE 3

Comparison of Prostate Diameter Measurement

	Reader 1: Radiologist			Reader 2: Physicist		
	1.5 T Endorectal	**3.0 T**	***P****	**1.5 T Endorectal**	**3.0 T**	***P****
Prostate Diameter Measurement						
Left-right (LR) [mm]	48.0 ± 6.0	48.1 ± 7.6	.553 (NS)	47.5 ± 5.6	45.7 ± 7.1	.039
Cranial-caudal (CC) [mm]	38.3 ± 6.0	43.2 ± 6.9	<.001	40.3 ± 5.7	42.1 ± 7.6	.179 (NS)
Anterior-posterior (AP) [mm]	26.2 ± 5.5	35.0 ± 5.9	<.001	25.5 ± 6.0	32.8 ± 6.3	<.001
LR/CC ratio	1.27 ± 0.18	1.13 ± 0.19	<.001	1.19 ± 0.17	1.10 ± 0.18	<.001
LR/AP ratio	1.88 ± 0.30	1.40 ± 0.23	<.001	1.93 ± 0.36	1.41 ± 0.19	<.001
Image Quality Scoring Result						
Posterior Border	4.48 ± 0.86	4.58 ± 1.04	.041	4.83 ± 0.38	4.81 ± 0.45	.946 (NS)
SV	4.51 ± 1.03	4.34 ± 1.09	.069 (NS)	4.75 ± 0.58	4.28 ± 0.77	<.001
NVB**	3.49 ± 0.83	3.63 ± 0.82	.101 (NS)	3.70 ± 0.58	3.69 ± 0.58	.869 (NS)
Overall Image Quality	4.19 ± 1.04	4.47 ± 1.04	.014	4.77 ± 0.48	4.64 ± 0.58	.107 (NS)
AUCs for Diagnostic Performance						
Sextant Tumor Localization	0. 5664	0. 5521	.701 (NS)	0.6095	0.5932	.628 (NS)
Extracapsular Extension	0. 7206	0.7250	.968 (NS)	0.6334	0.4475	.088 (NS)
SV Involvement	0. 5112	0.7714	.133 (NS)	0.5577	0.5625	.975 (NS)

NS, not significant.

SV, seminal vesicles

* P < .05 is considered statistically significant.

** Visualization of NVB was scored from 1 to 4. The other aspects were scored from 1–5. Higher score means better quality.